Electron Transfer Reaction in Infrared Organic Microcavities

By

Wajahat Hussain

Department of Physics,
Quaid-i-Azam University, Islamabad

A Dissertation submitted in the partial fulfilment of the requirements for the Degree of Maters of Philosophy in the Department of Physics Quaid-i-Azam University, Islamabad.

DECLARATION

I, Mr. **Wajahat Hussain** Roll No.**02182111021**, student of M.Phil. in the department of Physics session 2021-2023 here by declare that the matter printed thesis entitled **"Electron Transfer Reaction in Infrared Organic Microcavities"** is my review work and has not been printed, published or submitted as research work, thesis or publication in any form in any University, Research Institution etc. in Pakistan.

RESEARCH COMPLETION CERTIFICATE

This thesis submitted by **Wajahat Hussain Reg.No 02182111021**, is accepted in its present form by the Department of Physics. It satisfies the thesis requirements for the degree of Master of Philosophy in Physics.

Supervisor
Dr. M.Ahsan Zeb
Assistant Professor,
Department of Physics,
Quaid Azam Univeristy, Islamabad.

Chairman
Dr. Kashif Sabeeh
Professor,
Department of Physics,
Quaid Azam University, Islamabad.

DEDICATION

Dedicated to my **Parents** and beloved brother **M.Hussain**$_{(late)}$

Acknowledgments

All praises and thanks to Allah Almighty, who blessed me with the courage, health and consistency to make this journey possible.
First and foremost, I would like to express my deepest appreciation to my thesis advisor, **Dr. M.Ahsan Zeb**. Your guidance, expertise, and unwavering support have been invaluable throughout the research process.
I would like to thanks **Prof.Dr.Raheel Ali** for his invaluable support, encouragement and guidance throughout my academic years in **QAU**.
I extend my heartfelt thanks to my family for their unwavering support and understanding during this demanding period. I would like to thanks my brothers **Amjad, Mushtaque** and **Sajid** and my beloved sisters, your support, love and encouragement provided the foundation upon which I could build my academic pursuits. A special thanks to cousin **Engr.M.Ajmal Khan** who is always there for any discussion and support from the beginning.
Lastly but not least, I would like to acknowledge all my friends who are always there for me through every thick and thin and whose friendship I cherish the most.

Wajahat Hussain

Abstract

Recently, it is experimentally observed that the kinetics of charge transfer reactions in organic molecules can be modified by placing them inside an optical cavity and achieving the vibrational strong coupling (VSC). We review a theoretical study of the effect of matter-light coupling on the charge transfer reaction in organic molecules. We consider a disordered ensemble of N molecules coupled strongly to a resonant cavity and show how the optically vibrational dark states can alter the rate of charge transfer reactions. It is observed that a considerable increment is achieved when the electrons transfer reaction is carried under vibrational strong coupling.

Contents

List of Figures

Chapter 1

Introduction

Microcavities are tiny optical structures that are used to confine and control light at the micro- or nanoscale. They are formed by a a small, empty space, that is surrounded by two highly reflecting mirrors or material with a high refractive index. The size of the cavity is on the order of the wavelength of light, and it can trap the light inside, allowing it to interact with the surrounding material in unique ways. This interaction can result in the enhancement or suppression of certain optical properties.
When an organic material is placed inside in such a structure, it becomes organic microcavity. When the given transitions are in resonant with cavity mode, this can enhance the interaction of light with the organic material. This can lead to various changes in the physio-chemical properties of organic materials, electrons transfer rate is one of them.

A series of recent experiments has shown that chemical reactivity can be changed when a chemical mixture is placed inside an optical cavity [1]. An optical micro cavity is comprise of two mirrors which are highly reflective and the mirrors are adjusted to be parallel and are separated by a length of microscopic order, that ranges in between hundreds of nanometer to tens of micrometer. An analogous to the standing wave of sound in flute the standing wave of light can be supported by the cavity. Similar to the musical instruments, the standing waves formed in the cavity modes has a frequency that varies inversely proportional to the length of cavity.

The length of cavity can be adjusted in such a way that mod of cavity and vibrational or electronic transitions of molecules can be in resonant with each other. A favourable condition for the interaction of cavity and molecule is achieved by such kind of resonance. If the concentration of molecules is increased the interaction becomes enough stronger, the cavity mode will interact with the bright superposition of molecular transition, this results in the formation of particles or matter light states called the polaritons [2, 3].This kind of phenomenon is termed as strong matter light coupling (or strong coupling simply).

In experiments [1, 2, 4, 5] collective coupling between cavity mod and $N >> 1$ molecular transition is seen, where each transition inhabits in an individual molecule. As a result of such coupling two polaritons and $N - 1$ optically dark superposition's are formed.

the polaritons have partial photonic nature,so they have different energies than that of bare molecular states. These polariton states can also can be used a tool for the modification in chemical reactions. In fact polariton chemistry has emerged as a new field in the chemistry under strong matter light coupling in the recent past decades [1, 2, 6, 7]. Particularly the strong coupling of molecular vibrations or vibrational strong coupling has been considered as an attractive way to alter the kinetics of chemical reactions in in a wide range[1], that ranges from organic [8–10], inorganic [11] to enzymatic [12] chemical reactions.

Transition State Theory [13] have been applied on multiple studies to investigate the experimental changes in reaction rates because of the vibrational strong coupling (VSC), as transitional state theory is considered to be one of the most elementary and usually used theories of reaction rates, in the case of systems inside the micro cavities. However a negligible change in the reaction rate is shown by theoretical efforts when a system of many molecules collective experiences VSC with a cavity mod, as also in the experiments. This discrepancy is due to the fact that when VSC is achieved only 2 polaritons are formed as compared to that of $N - 1 >> 1$ dark states, and the energy of dark sates is same as that of bare vibrational states.

1.1 Organic Molecular Vibrations

A molecular vibration is a relative motion of atoms of molecules, which is assumed to be periodic in nature. In the molecular vibrational motion the center of mass remains unchanged. Typically the frequencies of vibrations are in the range less than $10^{13}\ Hz$ to almost $10^{14}\ Hz$, this range correspond to the wavelength 30 to $3\mu m$ and corresponding wavenumbers between 300 cm^{-1} and $3000cm^{-1}$.

Usually, normal modes are used to describe the molecular vibrations of polyatomic molecules, the normal modes are independent of each other. Generally, non-linear and linear molecules have $3N-6$ and $3N-5$ normal modes respectively. In linear molecules the rotation about the molecular axis cannot be observed, so that why they have one less normal mode than that of non-linear molecule's. Since the diatomic molecules either stretches or compresses, so that's why they posses only one normal mode.

When an energy ΔE , corresponding to the molecular vibrational frequency ω_v is absorbed by molecule, the molecular vibration is excited, according to the well known relation $\Delta E = \hbar\omega_v$. Excited states are higher energy levels. Energy gape between vibrational states correspond to infrared region of the light spectrum. So, therefore infrared spectroscopy allows us to examine the energy gape between ground state and excited sate and other higher states too. Transition from the vibrational ground state to first excited state denoted as $(E_0 \rightarrow {}_|E_1)$is termed as fundamental transition, while transition to higher excited states for instance $(E_0 \rightarrow E_2)$ is known as overtones.

For a diatomic molecule, the molecular vibrations can be modeled as simple harmonic oscillator (SHO) or mass spring system, where atoms of the molecule act as mass, strength of the bonds corresponds to the spring constant and relative change in bond length corresponds to the position in mass spring system in SHO.

Beyond the diatomic molecules, the molecular vibrations becomes complex, as more atoms are added to the molecule, so more elementary bands are seen. The molecule may undergo any of the following vibrational motion depending upon nature of bonding and molecule,

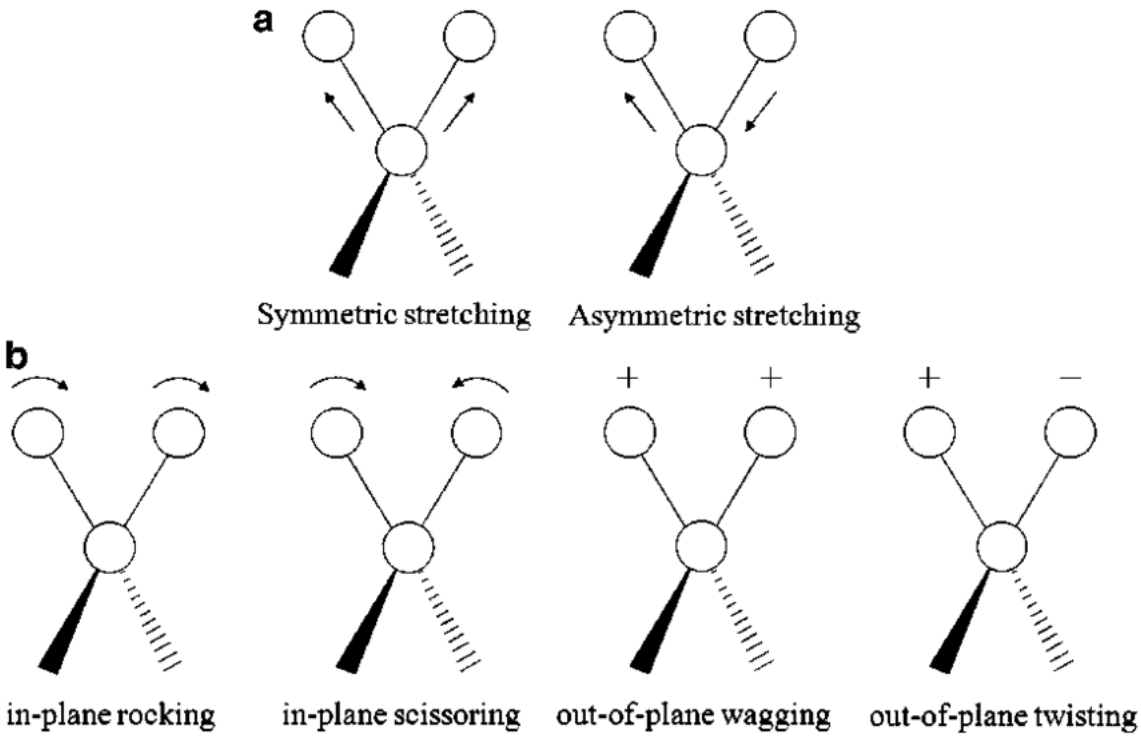

Figure 1.1: Possible Molecular vibrations

Symmetrical Stretching

Symmetrical stretching is simultaneous vibration of two bonds, in which bonds relaxes and contracts together.

Asymmetrical Stretching

In this kind of vibration one bond compresses while the other bond stretches at the same time.

Bending

In this kind of vibration the bond angle between two bonds changes.

1.2 Matter Light Interaction

A quantum electrodynamical or quantum transition by electrons that is accompanied by the absorption, emission or scattering of quanta of the electromagnetic field in vacuum i.e the photon is termed as matter light interaction or matter light coupling. To study the phenomenon of matter light coupling, micro-cavities are used, where a quantized light field interacts with matter in a small space that is confined. A microcavity [14] is a structure that is shaped to create resonant modes of electromagnetic field. The simplest toy model of this design is pair of highly reflective mirrors which are separated at small distance.

The matter light coupling strength is given as $g = \mu.E_0\sqrt{\frac{\omega_c}{2\epsilon V}}$, here E_0 is amplitude of radiation field, V is effective volume, μ is transition dipole moment and ϵ being the dielectric constant of cavity medium.

1.3 Weak and Strong Coupling

Consider an atom and cavity field interaction, there exist a dissipation i.e losses (ζ_c) and dephasing of atom (ζ_{at}), if the coupling strength (g) between cavity and atom is smaller as compared to the dissipation (i.e $g < \zeta_c,\ \zeta_{at}$) it turns out to be weak coupling. In this case there is small exchange of energy between cavity and atom takes place and they can be dealed as individual entities.

While if the coupling strength is greater than dissipation (i.e $g > \zeta_c,\ \zeta_{at}$) this in known strong coupling regime. Here atom and cavity field cannot be described as separate entities. Rapid energy exchange between atom and cavity takes place, that leads to the formation hybrid atom-cavity sates polaritons.

1.4 Electron Phonon Coupling

Phonons are quanta of vibrational energy that propagate as waves in solids, liquids, and other materials. They are similar to photons, which are quanta of electromagnetic energy that propagate as waves in vacuum. Phonons play a key role in determining the physical properties of materials, such as thermal conductivity, elasticity, and electrical conductivity.
In a quantized system electron-phonon coupling is described by

$$\mathcal{H} = H_e + H_p + H_{ep}, \tag{1.1}$$

electronic energy is represented by H_e while that of phononic is by H_p, H_{ep} represents the coupling between the electronic and phononic degrees of freedom.

$$H_e = \sum_k \hbar\omega_k c_k^\dagger c_k,$$

$$H_p = \sum_j \hbar\omega_j b_k^\dagger bj$$

$$H_{ep} = \hbar \sum_{k,j} g_j (c_k^\dagger b_j + h.c),$$

$c_k^\dagger(c_k)$ and $b_j^\dagger(b_j)$ are creation (annihilation) operators of electrons and phonons respectively where as their corresponding are represented as ω_k and ω_k, as g represents the coupling strength.
The electron-phonon interaction is an important factor in determining the electronic and thermal properties of materials, particularly in superconductors, where the interaction leads to the pairing of electrons and the formation of Cooper pairs. The study of the electron-phonon interaction is a crucial aspect of condensed matter physics and materials science.

1.5 Jaynes - Cummings Model

This is a quantum mechanical model used to which describes interaction between quantized light and two level system of atom. The model was first

introduced by American physicist Edwin T. Jaynes and British physicist Francis W. Cummings in 1963. To describe this model its Hamiltonian is written as

$$H_{JC} = \omega_c b^\dagger b + \omega_x \sigma^\dagger \sigma + g(b^\dagger \sigma + \sigma^\dagger b), \tag{1.2}$$

where $b^\dagger(b)$ and $\sigma^\dagger(\sigma)$ are raising (lowering) operators of cavity and two level system respectively. Transition frequency between two level is ω_x, cavity frequency is ω_c and g is matter light coupling strength.

Chapter 2

Electron Transfer In Infrared Organic Microcavities : Effect of Dark States

2.1 Introduction

Control of charge transfer phenomena through strong coupling of matter and light has been a point of interest in the recent past decades [2, 3, 15]. Vibropolaritonic chemistry is one of an exciting and inspiring prospect in this regard, that is nothing but the use of vibrational strong coupling to alter the reactivity of thermally activated charge transfer reactions in the absence of external source (i.e laser pumping). A large number of molecules involve in VSC, a sizeable change in the chemical kinetics of cycloaddition [10], organic substitution [16] , enzyme catalysis[17], hydrolysis [11] and crystallization[18] has been witnessed.

However, such kind of reactivity modification is not completely understood yet. Studies [19, 20] reveal that most commonly used configuration transition state theory (TST) cannot explain such kind of reaction kinetics well. Breakdown of TST counting, recrossing the activation barrier [21] , nonadiabatic/quantum phenomenon[22–24] and deviation from thermal equilibrium [25] have also been under consideration. These mentioned phenomenons de-

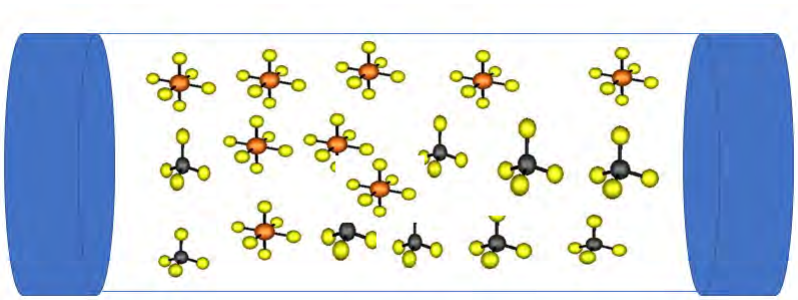

Figure 2.1: Symbolic of model setup.

mands all the N vibrations interacting or coupled to cavity mode needs to be identical. This assumption leads to the formation of two polaritons and $N-1$ dark vibrational modes.

Figure (2.1) shows a symbolic of model setup. A number of molecules are placed inside a cavity, where a cavity mode collectively couple to the molecular vibrations. The cavity coupled vibrational mode a molecule is slightly displaced, when the molecule under goes intermolecular electron transfer reaction. such kind of processes are studies in this work.
Here in this work it is shown that when disordered ensemble of molecules goes under vibrational strong coupling, a considerable change in the kinetics of thermally activated electron transfer reactions occurs.

2.2 Tavis-Cummings Model

Consider ensemble of N disordered molecular vibrations, inside an optical as shown in Figure (2.1). The system is described by the Hamiltonian

$$H = \hbar\omega_c a_0^\dagger a_0 + \hbar \sum_{i=1}^{N} \omega_i a_i^\dagger a_i + \hbar \sum_{i=1}^{N} g_i (a_i^\dagger a_0 + h.c) \tag{2.1}$$

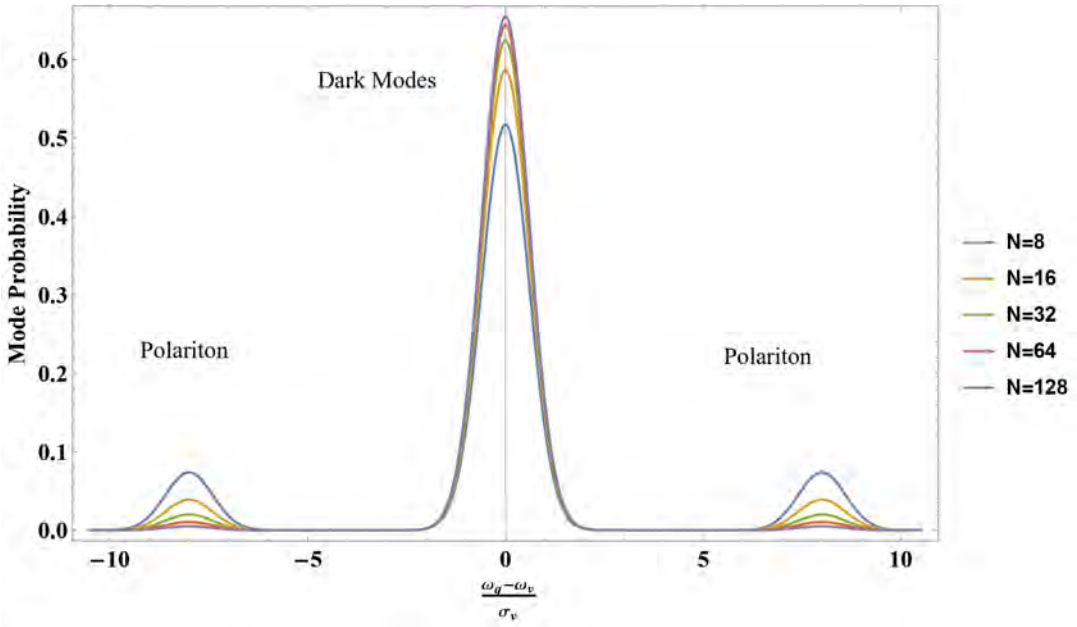

Figure 2.2: Probability distribution of Eigenmodes of Tavis-Cummings Model. The central peak of the graph shows dark modes, while the left and right small peaks ploraitons.

.

The ith vibrational mode has frequency $\omega_i = \bar{\omega_v} + \delta\omega_v$, where the mean vibrational frequency is represented by $\bar{\omega_v}$. Reflecting inhomogeneous broadening (static diagonal disorder), $\delta\omega_i$ is a random variable, that is normally with zero mean and σ_v standard deviation. The creation and annihilation operators of vibrational mode are represented by $a_i^\dagger$ and a_i and that of cavity mode are are given by $a_0^\dagger$ and a_0 respectively. The cavity mode has frequency ω_c , and couples to the ith vibrational mode with a coupling strength of g_i. For the simplicity we cab take assume all g_i to be the same i.e $gi = g$.

Using the Hamiltonian H for a system of disordered molecules that are under VSC, we tried to study the physio-chemical properties. In the all the calculations that are carried out it is assume that the cavity is in resonant with the mean vibrational frequency i.e $\omega_c = \bar{\omega_v}$ and the collective coupling strength between vibration is $g\sqrt{N} = 8\ \sigma_v$ for all N.

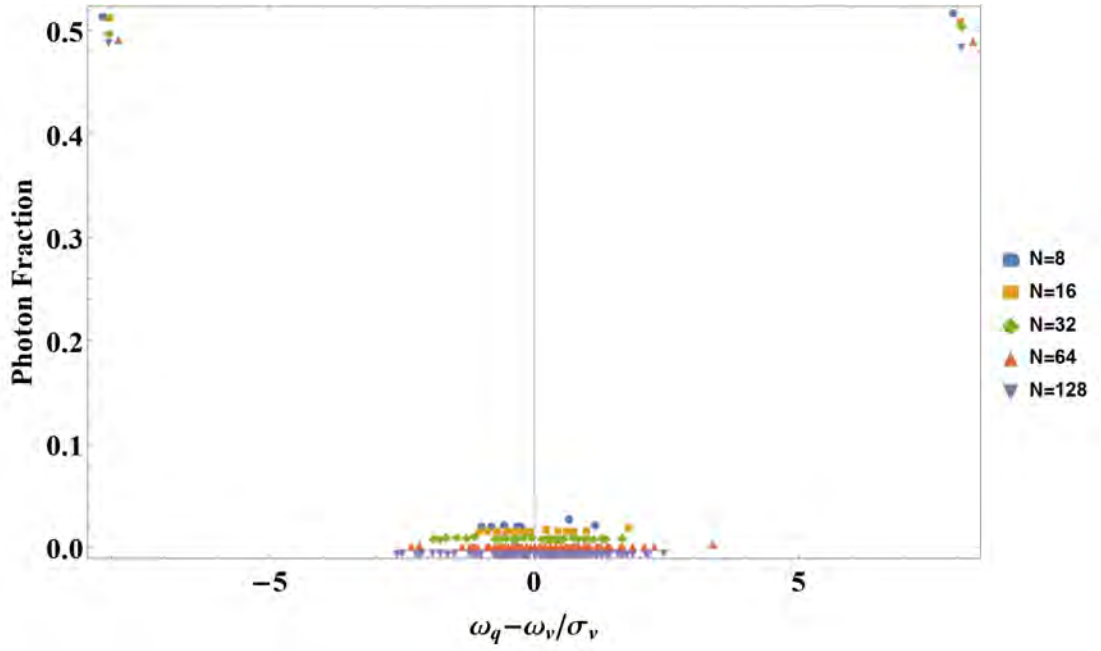

Figure 2.3: Photon Fraction of Eigenmodes of H

2.3 Eigenmodes of Tavis-Cummings Model

We first study the eigenmodes of H. The operator $\alpha_q = \sum_{i=0}^{N} c_{qi}$ represents the mode $q = 1, ..., N+1$, and the eigenmode q has frequency ω_q. Photon fraction $|c_{q0}|^2$ and probability distribution of eigenmodes are w.r.t eigen frequencies are shown in Figure (2.2 and 2.3)

Most of the modes are dark optically, an their frequencies forms a broad distribution around the mean vibrational frequency i.e $\bar{\omega_v}$. Few of the modes are bright i.e polaritons, and they have frequency which is differ from that of dark modes, this frequency lies in the range of $\bar{\omega_v} \pm 8\sigma_v$. As the number of molecules N is increased the number of dark modes also increases, i.e the probability of dark modes is higher for a large ensemble.

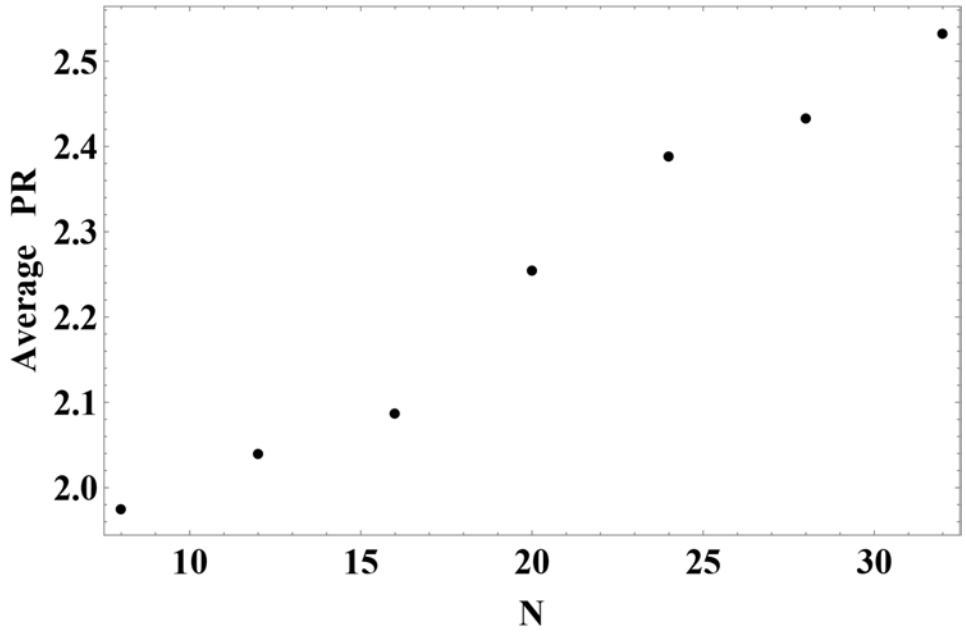

Figure 2.4: Participation ratio as function of N, for various N

2.3.1 Participation Ratio

To investigate the dark mode delocalization we study the phenomenon of participation ratio (PR). This is given as

$$PR = \frac{\mathcal{N}}{\sum_{i=1}^{N} |c_{qi}|^4}, \tag{2.2}$$

where $\mathcal{N} = \left| \sqrt{\sum_{i=1}^{N} |c_{qi}|^2} \right|^4$.
The participation ratio (PR) of an eigenstate is a measure of the number of basis states that contribute to the given eigenstate. A high PR value indicates that a large number of basis sates contribute to the given eigenstate, while a low PR value indicates that only a few basis states contribute to the eigenstate. In other words, the PR provides information on the spatial localization of the state and is often used as a measure of disorder in a system.

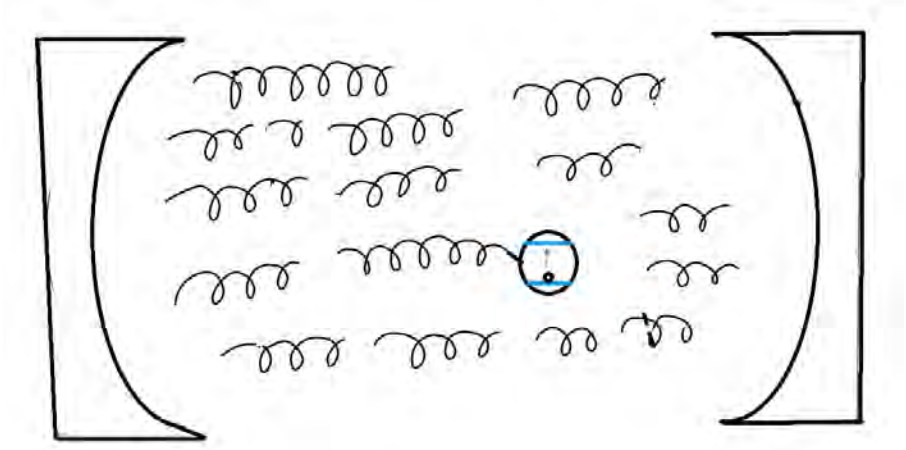

Figure 2.5: Inside an optical cavity the vibrational modes are coupled to cavity and reactive mode is coupled to electronic states i.e ($|R\rangle$ and $|P\rangle$)

2.4 Electron Transfer Reaction

When a charge particle i.e electron migrates from one specie to another this mechanism is electron transfer reaction. Such kind of mechanism leads to oxidation reduction processes. Here in this section we are going to study the influence of VSC on the kinetics of charge transfer reactions. As shown in Figure (2.1 and 2.5) a molecular ensemble is placed inside the cavity where a reactive molecule goes under Vibrational strong coupling. A non-adiabatic intramolecular electron transfer takes place.

2.4.1 Hamiltonian

In the ensemble, the reaction of one molecule can be modeled by using the Hamiltonian H_{rxn} , where

$$\begin{aligned} H_{rxn} = \hbar\omega_c a_0^\dagger a_0 + \hbar\sum_{i=1}^{N}\omega_i a_i^\dagger a_i + \hbar\sum_{i=1}^{N} g_i(a_i^\dagger a_0 + h.c) \\ + \sum_{X=R,P} |X\rangle\langle X|\{E_X + \hbar\omega_r[\lambda_X(a_r + a_r^\dagger)]\} + \Delta_S. \end{aligned} \tag{2.3}$$

Here,$|X\rangle$ refers to the electronic states reactant and product denoted as

$|R\rangle$ and $|P\rangle$ respectively. The bare vibrational mode index ($i = 1$) involved in the reaction is represented as v_r or we can write as ($a_1 \rightarrow {}_{|}a_r \;\; \omega_1 \rightarrow \omega_r$). E_X is energy of electronic state $|X\rangle$ that interacts with the reactive mode v_r with a coupling strength λ_X, which is a dimensional less quantity.The Vibronic coupling compels reactive mode v_r to displace from its equilibrium position when the electron transfer takes place.
Δ_s in Equation (2.3) represents reorganization energy that arise due to the small frequency vibrations and small perturbations. In this electron transfer system under VSC, we have considered no direct coupling between cavity and electronic state i.e $|R\rangle \rightleftharpoons |P\rangle$ is dipole forbidden.

2.4.2 Kinetic Model

In our model the reactant and product are connected through a small perturbation so the entire charge transfer carried out is nonadiabatic. We calculate the reactive transition rates using the Hamiltonian H_{rxn}. The eigenstates of Hamiltonian H_{rxn} can be written as $|X, \chi\rangle = |X\rangle \otimes |\chi\rangle$. Where, $|X\rangle$ and $|\chi\rangle$ represents electronic and vibrational-cavity states.
A displacement operator $D_q(\lambda) = \exp(\lambda \alpha_q^\dagger - \lambda^* \alpha_q)$ when is applied to an undisplaced Fock state $|\chi\rangle$, the state is displaced and a new state is formed i.e $|\bar{\chi}\rangle = (\Pi_{q=1}^{N+1} D_q^\dagger(\lambda_{Xq})|\chi)$, which has $m_q^{(\chi)}$ excitation's in q eigenmode of H. Equilibrium position of mode q in the $|X\rangle$ electronic state is given as

$$\lambda_{Xq} = \lambda_X c_{qr}(\omega_r/\omega_q).$$

The energy associated with vibrational-cavity-electronic state $|X, \chi\rangle$ is is given by

$$E_{(X,\chi)} = E_X + \sum_{q=1}^{N+1} m_q^{(\chi)} \hbar \omega_q + \Delta_X. \tag{2.4}$$

The last term in Equation (2.4) is reorganization energy difference that arises because of the vibronic interaction between v_r and $|X\rangle$, and that is

$$\Delta_X = \lambda_X^2 \omega_r - \hbar \sum_{q=1}^{N+1} |\lambda_{Xq}|^2 \omega_q.$$

These electron transfer reactions can be understand as population transfer from one state to another. Evolution of population is described by the master equation

$$\frac{dP_{(X,\chi)}}{dt} = - \sum_{(X,\chi)\neq(\bar{X},\bar{\chi})} K_{(X,\chi)\hookrightarrow(\bar{X},\bar{\chi})} P_{(X,\chi)} + \sum_{(X,\chi)\neq(\bar{X},\bar{\chi})} K_{(\bar{X},\bar{\chi})\hookrightarrow(X,\chi)} P_{(\bar{X},\bar{\chi})} \tag{2.5}$$

The K in Equation (2.5) shows the rate of population transfer. Modeling this to the electrons transfer reactions, the state to state population transfer can either be reactive, which includes forward and backward reactions or it may be non reactive. Transfers are said to be reactive if $X \neq \bar{X}$ and when $X = \bar{X}$ it will be called as non-reactive transfer.
Keeping the above evolution in mind and following the Marcus- Levich-Jortner theory [26, 27] which is most suitable for our model, the reactive transition rate of electron transfer under vibrational strong coupling is given as

$$K_{(R,\chi)\hookrightarrow(P,\bar{\chi})} = A F_{\chi,\bar{\chi}} \exp(-\beta E_a^{\chi,\bar{\chi}}), \tag{2.6}$$

here $A = \sqrt{\frac{\pi\beta}{\lambda_s}}\ |J_{PR}|^2/\hbar$, where λ_s and J_{PR} are associated with reorganizations energy corresponds to low frequency vibrations and small perturbation respectively and β is inverse of temperature for this reaction. The activation energy is given as

$$E_{\chi,\bar{\chi}} = (E_{(P,\chi)} - E_{(R,\bar{\chi})} + \lambda_s)^2/4\lambda_s.$$

The component $F_{\chi,\bar{\chi}} = |\langle\chi|\bar{\chi}\rangle|^2$ is known as Franck-Condon (FC) factor, which is nothing but an overlap between initial and final sates of vibrational

cavity space. The reactive transitions mainly depends on the FC, using the standard identity [28] we can calculate the $F_{\chi,\bar{\chi}}$ for our use we can write

$$\langle n|D(\lambda)|\bar{n}\rangle = \sqrt{\frac{\bar{n}!}{n!}}\ \exp\left(-\lambda/2\right)\ \lambda^{n-\bar{n}}\ L_{\bar{n}}^{(n-\bar{n})}(|\lambda|^2) \qquad n \geq \bar{n}, \tag{2.7}$$

where $D(\lambda)$ is displacement operator as explained earlier in this section, $|n\rangle$ is a number state and $L_l^m(k)$ is an associated Laguerre polynomial. Using Equation (2.7) different combinations of $F_{\chi,\bar{\chi}}$ can be calculated, some of them in our use are

$$\begin{aligned} F_{(0,0)} &= e^{(-S)}, \\ F_{(0,1_q),(1_q,0)} &= e^{(-S)}\ S_q, \\ F_{(1_q,1_q)} &= e^{(-S)}\ (1-S_q)^2, \\ F_{\substack{'\\(1_q,1_q)\\ q\neq q'}} &= e^{-(S)}\ S_q\ S_q^{'}, \end{aligned} \tag{2.8}$$

here $S = \sum_{q=1}^{N+1}\ Sq$ where $S_q = |\lambda_{Pq} - \lambda_{Rq}|^2$.
The non reactive transitions in the models are of two types, vibrational-cavity decay, and exchange of energy among polariton and dark states [29]. The second process arises due to vibrational dephasing. The cavity decay is given as

$$K_{(X,1_q)\hookrightarrow(X,0)} = |c_{q0}|^2\kappa\ \ +\ \ \gamma\sum_{i=1}^{N}|c_{qi}|^2, \tag{2.9}$$

here κ and γ represents cavity and bare vibrational decay respectively. The The reverse process of Equation(2.9) is given as

$$K_{(X,0)\hookrightarrow(X,1_q)} = K_{(X,1_q)\hookrightarrow(X,0)}\exp\left(-\beta\hbar\omega_q\right).$$

Relaxation among dark and polariton states, as suggested by [30, 31] is given as

$$K_{(X,1_q)\hookrightarrow(X,1_q')} = \mathcal{R}(\omega_q - \omega_{q'})\ \ \sum_{i=1}^{N}|c_{qi}|^2|c_{q'i}|^2, \tag{2.10}$$

$q \neq q'$ and

$$\mathcal{R}(\omega) = 2\pi[\phi(-\omega)(m(-\omega)+1)\mathcal{J}(-\omega) + \phi(\omega)m(\omega)\mathcal{J}(\omega)]. \tag{2.11}$$

Here $\phi(\omega)$ represents Heaviside step function, $\mathcal{J}(\omega)$ spectral density and $m(\omega) = [\exp(-\beta\omega) - 1]^{-1}$ is Bose-Einstein Distribution function.

2.4.3 Reaction Parameters

The parameter used throughout to calculate the kinetics of the reaction are described in this section.

As, the molecular ensemble goes under VSC, and the frequency of molecular vibrations lies infrared region, so the mean vibrational frequency is taken as $\bar{\omega_v} = 2000cm^{-1}$ which are evident from experimental studies [9, 10, 32]. The phenomena of inharmonious broadening is not studied in these studies, so we take a standard deviation of $\sigma_v = 10$ in mean vibrational frequency, this lead to the spectral line width of around $\approx 24cm^{-1}$ which is in tune with the line shape that is studied and cited in work [9, 10, 33]. We have chosen the cavity frequency in such a way that it is in resonant with the the mean vibrational frequency i.e $\omega_c = \bar{\omega_v}$ the coupling strength between cavity and vibrational modes is taken as $g\sqrt{N} = 8\sigma_v$ for all N. The other parameters that are involved in the simulations of reactions [25] are as

$E_R = 0, E_P = -0.6\bar{\omega_v}, \lambda_R = 0, \lambda_P = 1.5, J_{PR} = 0.01\bar{\omega_v}, \lambda_s = 0.08\bar{\omega_v}$.

There are some other parameters as well which governs the relaxation of cavity and vibrational modes. The reaction process is carried out at temperature $T = 298K$. We choose the bare cavity decay $\kappa = 1ps^{-1}$ and bare vibrational decay rate $\gamma = 0.01ps^{-1}$ [34] (for all bare vibrational modes).

Super Ohmic spectral density is used to model the relaxation among dark and polariton states that is

$$\mathcal{J}(\omega) = \eta\omega_0^{-1}\omega^2 \exp[-(\frac{\omega}{\omega_{cut}})^2]. \tag{2.12}$$

here $\eta = 1 \times 10^{-3}$ is coupling strength between each bare vibrational mode and local chemical environment, environmental modes have cutoff frequency

$\omega_{cut} = 50cm^{-1}$ and $\omega_0 = \omega_{cut}$.

Condensed-phase system[35] and liquid molecular system [36] resembles to the spectral density and cutoff frequency respectively.

The motivation behind the choice of spectral density is, firstly it allows the relaxation between dark and polaritons on the time scale $20 - 25ps$ around. Secondly, the relaxation rate between dark states decreases as the frequency difference between dark states approaches to zero, as shown in the figure in this section where it is can be seen that for ($\mathcal{J}$ $(\omega) \rightarrow 0$ as $\omega \rightarrow 0$).

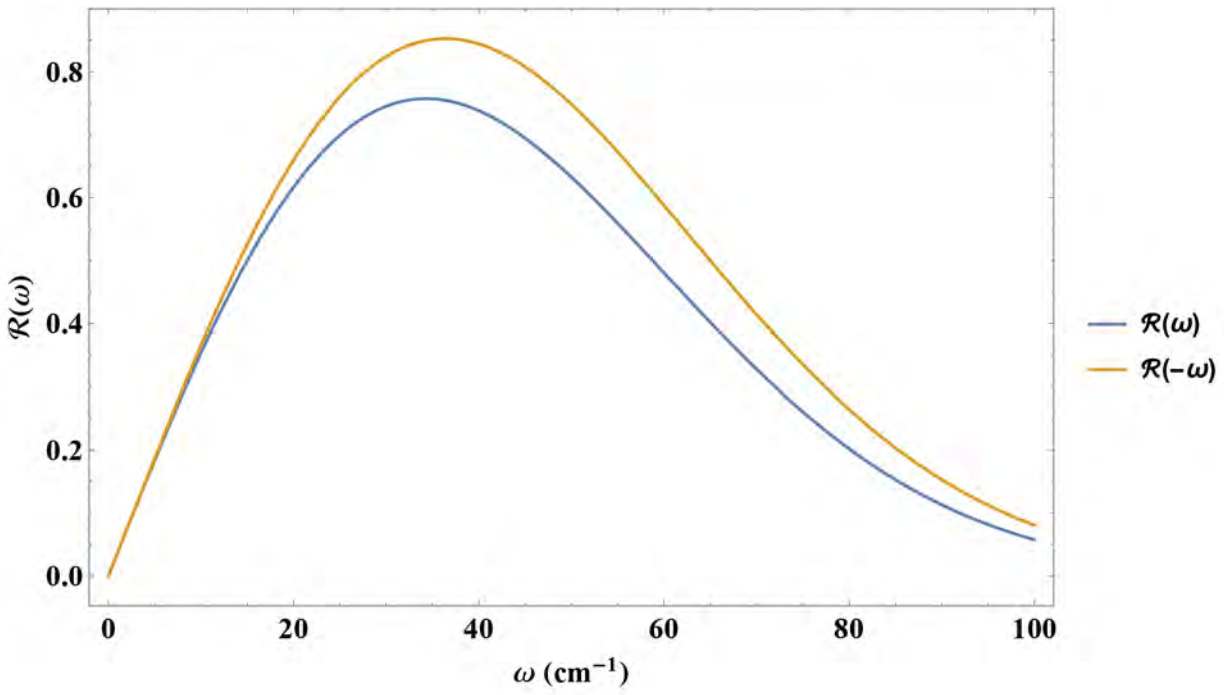

Figure 2.6: Graphical representation of Equation (2.11) for $\mathcal{J}(\omega)$ of Eqn.(2.12)

2.5 Approximate Kinetic Models for Electron Transfer Reactions

To obtain the numerical values of reaction rates we run the full numerical simulations.Here in this section we introduce the models that will help in the conceptual understanding of the reaction kinetics.

2.5.1 Bare Reaction and its Analytical Rate:

A symbolic representation of bare and VSC reactions is shown the Figure (3.7). The process begins as follow;
Assuming the system is in vibrational ground state, the reactions takes place i.e the reactant is converted into product mainly by the vibronic transition that's $0 \rightarrow 1$. This excites the reactive mode, as a result the reaction starts to occur, the rate at which the forward reaction takes place is denoted as $K_f \equiv K_{(R,0)\rightarrow(P,1_r)}$, using Equation (2.6) the rate of forward reaction (bare) is given as

$$K_f = AF_{0,1_r} \exp(-\beta E_a) \tag{2.13}$$

the activation energy $E_a \equiv E^{0,1_r}$. Once the product is formed, it starts to revert into the reactants with a backward reaction rate denoted as $K_b \equiv K_{(P,1_r)\rightarrow(R,0)}$ and $K_b >> K_f$, where the rate is given as

$$K_b = K_f \exp[\beta(E_p + \omega_r - E_R)] \tag{2.14}$$

the vibrational hot product may also decays with decay rate $\gamma \approx K_b$ to its vibrational ground state. When the product is in its vibrational ground state it do not take part in further reaction process because its reverse activation energy which is very high indeed.
To calculate the total reaction rate consider the simplified version of kinetic model, the population evolves with time as follow ;

$$\frac{dP_{(R,0)}}{dt} = -K_f P_{(R,0)} + K_b P_{(P,1_r)} \tag{2.15}$$

and the evolution of product population is gen as;

$$\frac{dP_{(P,1_r)}}{dt} = K_f P_{(R,0)} - (K_b + \gamma) P_{(P,1_r)} \tag{2.16}$$

The above both equations shows how the population of reactants and products changes with time. Consider the steady state approximation (SSA) to the product state $P_{(P,1_r)}$, where we assume all the state variable of system to be constant. So we can write it as $\frac{dP_{(P,1_r)}}{dt} \approx 0$ using the approximation the equation 2.16 can be written as

$$0 = K_f P_{(R,0)} - (K_b + \gamma) P_{(P,1_r)} \tag{2.17}$$

and we can write it as

$$(K_b + \gamma) P_{(P,1_r)} = K_f P_{(R,0)} \tag{2.18}$$

$$P_{(P,1_r)} = \frac{K_f}{(K_b + \gamma)} P_{(R,0)} \tag{2.19}$$

Plugging the above equation 2.18 into 2.15 it can be written as

$$\frac{dP_{(R,0)}}{dt} = -K_f P_{(R,0)} \quad + \quad K_b \frac{K_f}{(K_b + \gamma)} P_{(R,0)} \tag{2.20}$$

further more simplifying this can be written as

$$\frac{dP_{(R,0)}}{dt} = -K_f \left(1 - \frac{K_b}{K_b + \gamma}\right) P_{(R,0)} \tag{2.21}$$

further we can write it as

$$\frac{dP_{(R,0)}}{dt} = -K_f \left(\frac{\gamma}{K_b + \gamma}\right) P_{(R,0)} \tag{2.22}$$

Comparing 2.22 to $\frac{dP_{(R,0)}}{dt} = -K_{bare}^{analytical} P_{(R,0)}$ we can write

$$K_{bare}^{analytical} = K_f \left(\frac{\gamma}{K_b + \gamma}\right) \tag{2.23}$$

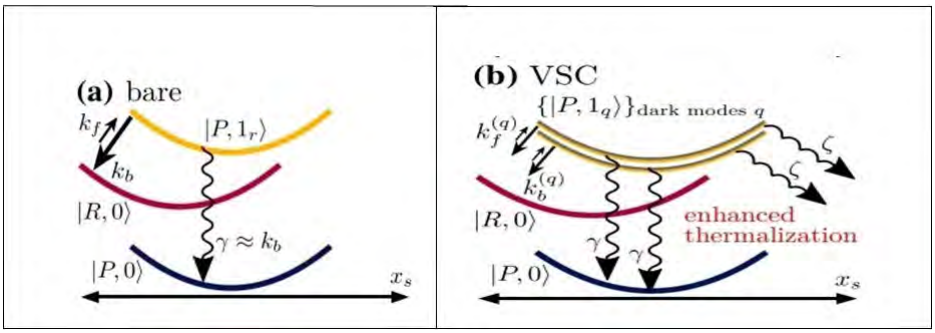

Figure 2.7: Schematic of bare (a) and VSC (b) reaction kinetics. Potential energy surfaces (PES) are represented parabolas.The forward and backward reactions are represented by straight arrows, while the curly arrows shows non reactive transitions and cavity losses.

is the net rate bare reaction rate.

2.5.2 Reaction Under VSC and its Analytical Reaction Rate

Under the influence of VSC the path followed splits into multiples of path, that is due to excitation and de-excitation of eigen modes i.e polariton and dark modes. Following the Equation (2.6), forward and backward reaction rates in the case of VSC are given as

$$K_f^{(q)} = AF_{0,1_q} \exp(-\beta E_a^{(q)}) \tag{2.24}$$

and

$$K_b^{(q)} = K_f^{(q)} \exp \beta(E_p - E_R + \Delta_P - \Delta_R + \omega_q) \tag{2.25}$$

respectively, the forward and backward reactions are described as $K_f^{(q)} \equiv K_{(R,0)\rightarrow(P,1_q)}$ and $K_b^{(q)} \equiv K_{(P,1_q)\rightarrow(R,0)}$ respectively, and the activation energy $E_a^{(q)} \equiv E_a^{(0,1_q)}$. As the size of ensemble N increases the the number of dark modes also increases, and they start to localize on bare mode. The overlap

of average bare with polariton modes diminishes i.e ($c_{qr} \propto \frac{1}{\sqrt{N}} \to 0$ for he polariton modes mainly represented by $q = 1, N+1$). This shows that the quantity $c_{qr} \not\approx 0$ for for those mode q which are dark. This mean that the activation energy for bare and dark mode is the same i.e

$$E_a^{(q)}|_{c_{qr} \not\approx 0} \approx E_a.$$

This shows that the only factor that has different value in both cases is the Franck-Condon (F-C) $F_{a,b}$. To compare the F-C see section (A.3), and for single mode under consideration we are now able to write

$$F_{0,1_q} \approx |c_{qr}|^2 F_{0,1_r},$$

using this relation to forward and backward reaction rates of both VSC and bare we can relate the rates as

$$K_{f/b}^{q} \approx |c_{qr}|^2 K_{f/b}^{(bare)}. \tag{2.26}$$

In the model, when the system goes under VSC, during the electron transfer process the polaritons are disassociated from reaction. The reaction goes on only due to the set of those modes which are dark. Let us define set dark modes $\mathcal{D}$ and $q \in \mathcal{D}$. Consider the population of reactant state $|R, 0\rangle$ which evolves as

$$\frac{dP_{(R,0)}}{dt} = -\sum_{q \in \mathcal{D}} K_f^{(q)} P_{(R,0)} \quad + \quad \sum_{q \in \mathcal{D}} K_b^{(q)} P_{(P,1q)} \tag{2.27}$$

and the product sate $|P, 1_q\rangle$ whose population changes as

$$\frac{dP_{(P,1q)}}{dt} = -(K_b^{(q)} + \gamma) P_{(P,1q)} \quad + \quad K_f^{(q)} P_{(R,0)} \tag{2.28}$$

To calculate the net reaction rate likewise bare reaction, here we can also use the SSA to the product population $P_{(P,1q)}$ i.e $\frac{dP_{(P,1q)}}{dt} \approx 0$. Using the

approximation, Equation (2.28) can be written as

$$(K_b^{(q)} + \gamma)P_{(P,1q)} = K_f^{(q)} P_{(R,0)}$$

$$P_{(P,1q)} = \frac{K_f^{(q)}}{K_b^{(q)} + \gamma} P_{(R,0)} \tag{2.29}$$

by putting Equation (2.29) into Equation(2.27) we get

$$\frac{dP_{(R,0)}}{dt} = -\sum_{q\in\mathcal{D}} K_f^{(q)} P_{(R,0)} \quad + \quad \sum_{q\in\mathcal{D}} \left(\frac{K_f^{(q)}}{K_b^{(q)} + \gamma} \right) K_b^{(q)} P_{(R,0)} \tag{2.30}$$

Further more simplification of Equation (2.30) leads to

$$\frac{dP_{(R,0)}}{dt} = -\sum_{q\in\mathcal{D}} K_f^{(q)} \left(\frac{\gamma}{K_b^{(q)} + \gamma} \right) P_{(R,0)}. \tag{2.31}$$

Using Equation (2.26) we can write the rate equation for VSC as

$$\frac{dP_{(R,0)}}{dt} = -\sum_{q\in\mathcal{D}} K_f \left|c_{qr}\right|^2 \left(\frac{\gamma}{\left|c_{qr}\right|^2 K_b + \gamma} \right) P_{(R,0)}.$$

Comparing above equation to $\frac{dP_{(R,0)}}{dt} = -K_{VSC}^{analytical} P_{(R,0)}$, we get

$$K_{VSC}^{analytical} = \sum_{q\in\mathcal{D}} K_f \left|c_{qr}\right|^2 \left(\frac{\gamma}{\left|c_{qr}\right|^2 K_b + \gamma} \right)$$

further it can be written as

$$K_{VSC}^{analytical} = K_f \left\langle \frac{\gamma}{\gamma \quad + \quad \left|c_{qr}\right|^2 \quad K_b} \right\rangle, \tag{2.32}$$

this is effective transition rate of system under vibrational strong coupling. Equation (2.32) clearly shows that its a weighted mean over all modes q that are dark (i.e $q \in \mathcal{D}$) and $\left|c_{qr}\right|^2$ is weight of each dark mode. Since, for all

modes q the weighted factor $|c_{qr}|^2 < 1$, that's

$$K_{VSC}^{analytical} > K_{bare}^{analytical}.$$

The above relation shows that under vibrational strong the charge transfer reaction has a higher rate then that of the same system in the absence of coupling i.e (bare g=0).

2.6 Numerical Results

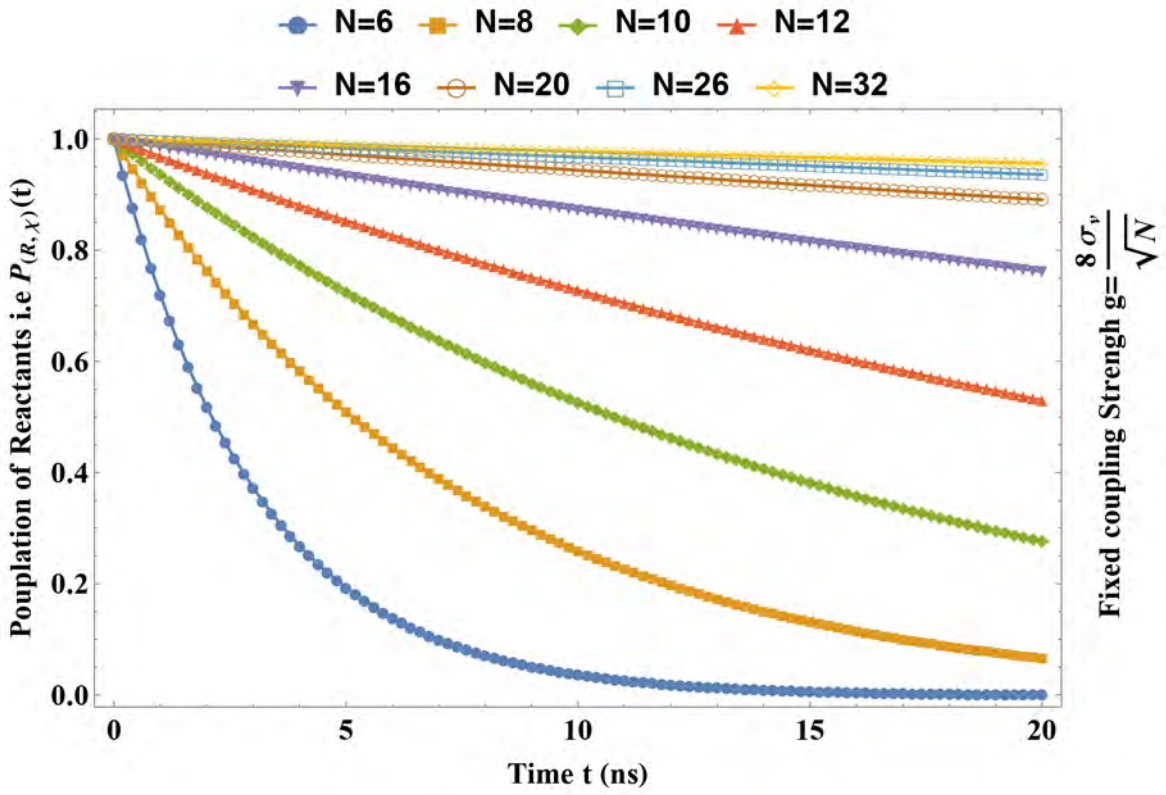

Figure 2.8: Evolution of reactant population for various N under VSC

Here in this section we will discuss the numerical results obtained in this work. Population transfer dynamic is studied while considering that vibra-

tional cavity mode has one or zero excitation , denoted as $\chi = 1_q$ and $\chi = 0$ respectively, here q represents the eigenmode of vibrational-cavity subspace.

In the process we have assumed that the initially the population is dis-

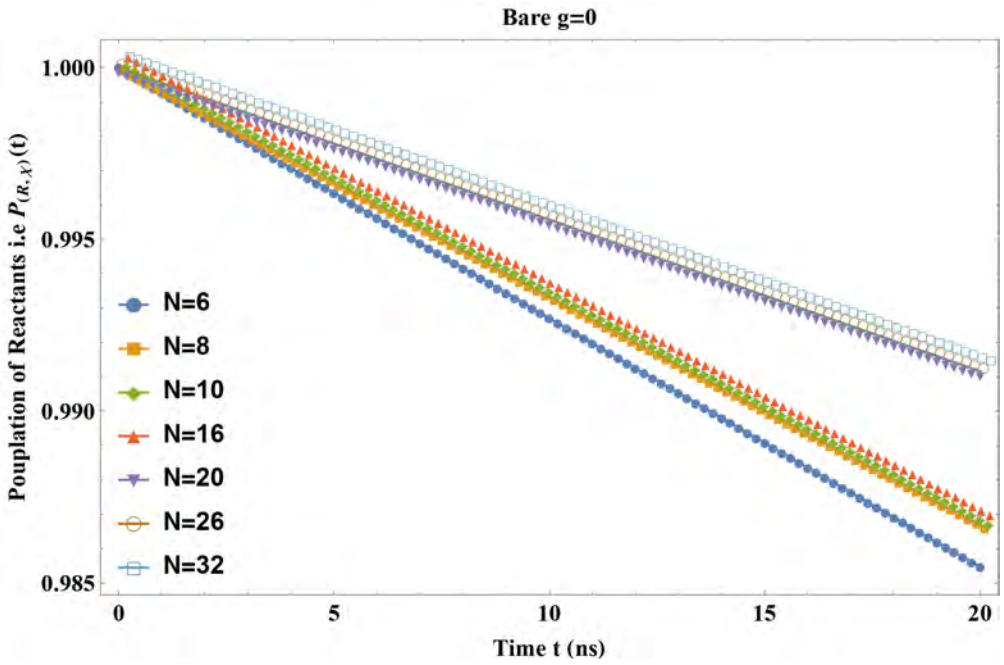

Figure 2.9: Evolution of reactant population for various N in the absence of coupling $g = 0$

tributed in reactant states $|R, \chi\rangle$. Using the method discussed in section (B.1) we obtained the numerical results for both VSC and bare ($g = 0$) case, which are shown in this section.

Figures (2.8, 2.9) are population vs time graphs, that shows how the population of reactants changes with time. Both of the figures shows at time $t0 =$ the reactant populations $R_{R,\chi}(0) = 1$, show that initially the population is distributed in reactant state.

We than calculated net rates of reaction for both of the cases i.e VSC and bare. Ratios of reaction rate denoted as K_{VSC}/K_{bare} shows the ratio of rate of reaction under vibrational strong coupling to that of bare. Rate ratios for various ensemble (i.e number of molecules N) are shown in this section. The

graph of reaction rate ratio is shown in Figure (2.10), that shows reaction rate ratio of VSC to the bare is greater than one for all all the size of ensemble taken under consideration.

We also look into the effect of cavity detuning on kinetics of our system

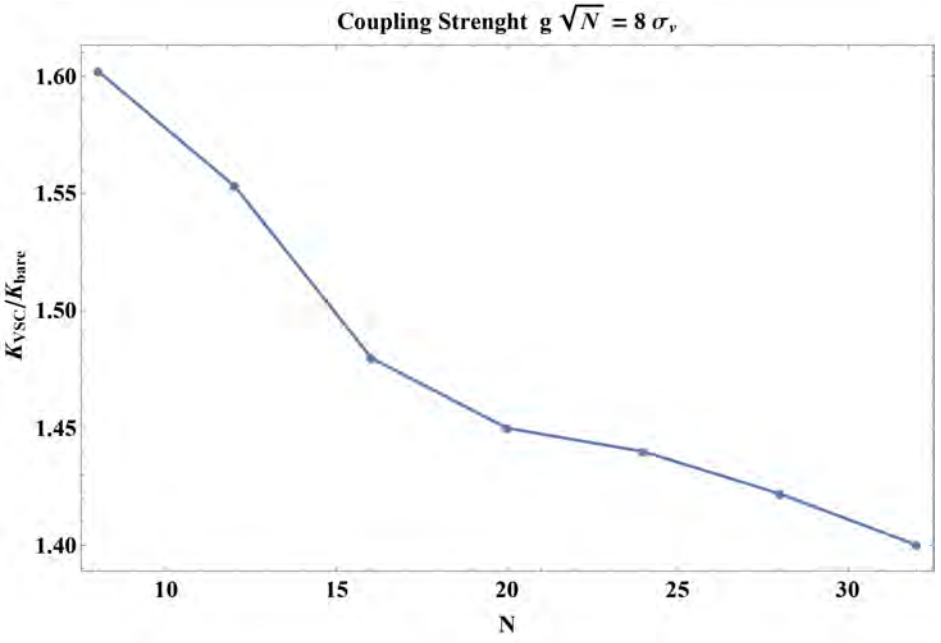

Figure 2.10: Reaction rate ratios K_{VSC}/K_{bare} for various N and fixed coupling strength.

under consideration. Cavity detuning refers to a change in the frequency of the light in a microcavity from its resonance frequency $\delta = \omega_c - \bar{\omega_v}$. Also delocalization of reactive mode, defined as $v_r = 1/\sum_{q=1}^{N+1}|c_{qr}|^4$, for various coupling strength is studied in this work. Figure (2.11, 2.12) shows graphical representation of K_{VSC}/K_{bare} and reactive mode delocalization as function of cavity detuning for various coupling strengths by keeping the size of ensemble $N = 32$ fixed.

The obtained numerical values and their corresponding graphs shows that the reactive mode delocalization is maximum at resonance and decreases with detuning. Also by keeping the coupling strength constant we investigated the effect of cavity detuning in reaction rates of various size of ensemble, which are also shown in Figure (2.13).

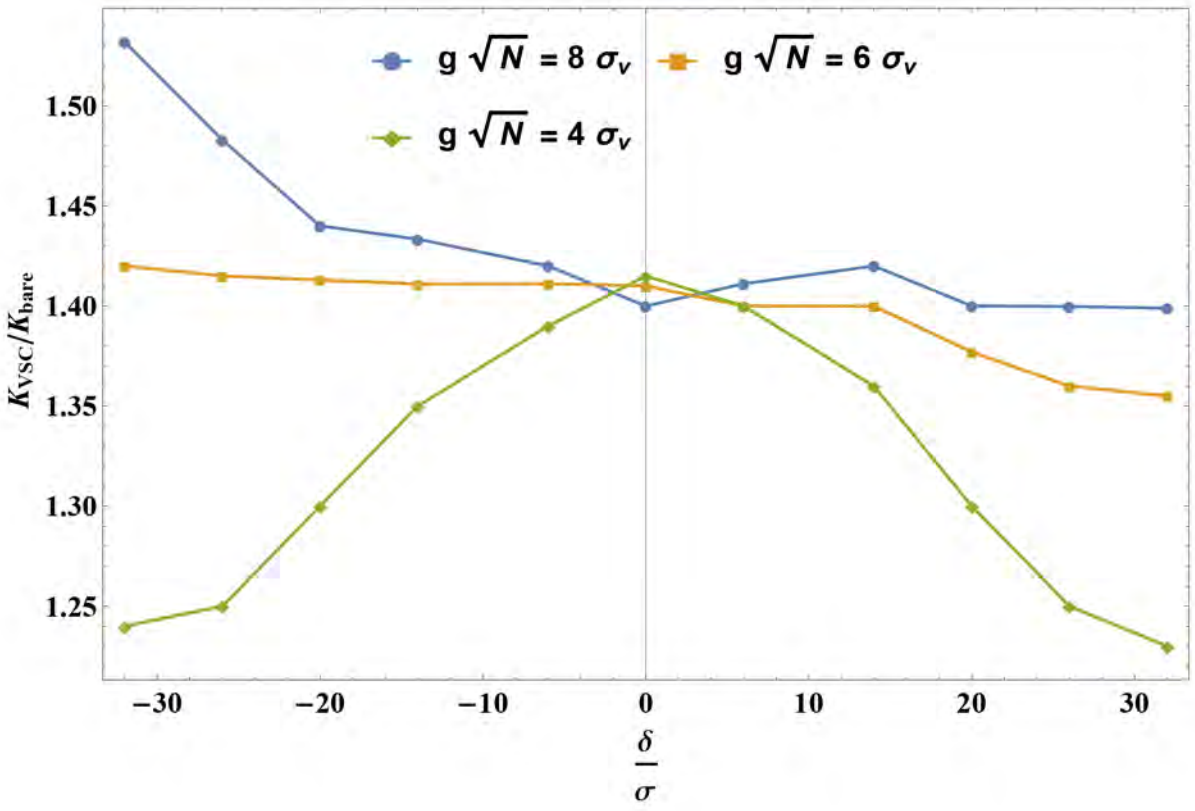

Figure 2.11: K_{VSC}/K_{bare} as function of cavity detuning for fixed $N = 32$ and various coupling strength.

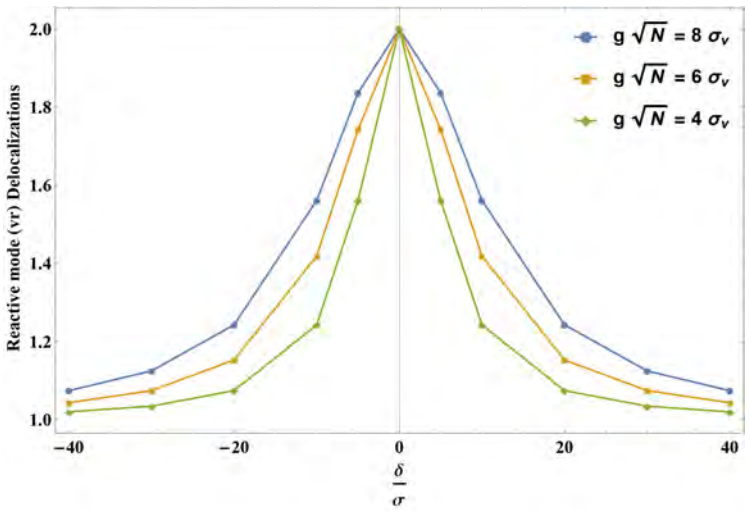

Figure 2.12: vr delocalization as function of cavity detuning or various coupling strengths and fixed $N = 32$.

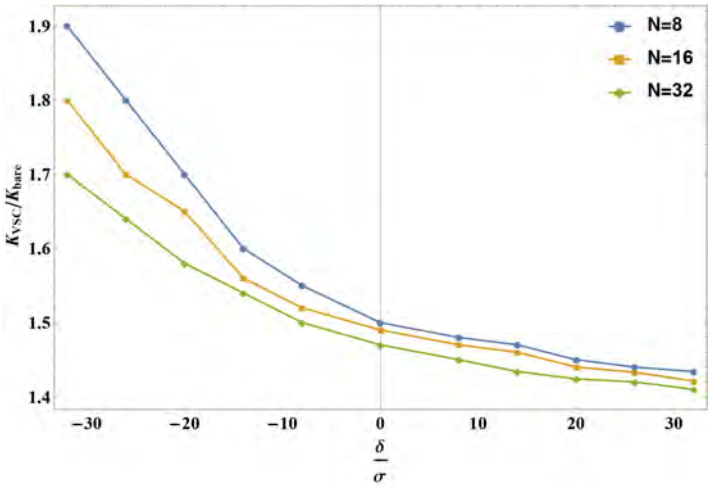

Figure 2.13: K_{VSC}/K_{bare} as function of cavity detuning for different N and constant coupling $g\sqrt{N} = 8\sigma_v$.

Chapter 3

Conclusion

We studied the effect vibrational strong coupling on electron transfer reaction and compared it with that of bare. Finally we reached at the result that by semi-localizing dark modes the disordered molecular ensemble under VSC can alter the kinetics of thermally activated reaction. We noticed that a significant change in the kinetics of thermally activated reaction can occur when reaction is carried out under vibrational strong. In our entire calculations we noticed that productivity rate can be increased by around 50% when VSC mechanism is taken under consideration.

We also investigated the desired results under various coupling strengths and found that the ratio K_{VSC}/K_{bare} always great than one ($K_{VSC}/K_{bare} > 1$). Moreover we studied the effect of cavity detuning on reaction rates and found the similar behaviour for various values of detuning. By repeating the same procedure under various coupling strengths we found that the ratio ($K_{VSC}/K_{bare} > 1$). This show that under vibrational strong coupling a considerable increment in the rate of electron transfer reaction can be achieved.

Appendix A

A.1 Matrix Representation of T-C Model

	P	χ_1	χ_2	χ_3	χ_4	.	.	.	χ_n
P	ω_c	g1	g2	g3	g4	.	.	.	gn
χ_1	g1	ω_1	0	0	0	0	0	0	0
χ_2	g2	0	ω_2	0	0	0	0	0 0	0
χ_3	g3	0	0	ω_3	0	0	0	0	0
χ_4	g4	0	0	0	ω_4	0	0	0	0
.	.	0	0	0	0	.	0	0	0
.	.	0	0	0	0	0	.	0	0
.	.	0	0	0	0	0	0	.	0
χ_n	gn	0	0	0	0	0	0	0	ω_n

A.2 Properties of Displacement Operator

$$D_q(\lambda) = \exp(\lambda\alpha_q^\dagger - \lambda^*\alpha_q)$$

$$D^{-1}(\lambda) = D^\dagger(\lambda)D(-\lambda) \tag{A.1}$$

$$D^\dagger(\lambda)G(a,a^\dagger)D(\lambda) = G(a+\lambda, a^\dagger+\lambda^*) \tag{A.2}$$

$$D(\lambda)D(\beta) = D(\lambda+\beta)\exp[\frac{1}{2}(\lambda\beta^* - \lambda^*\beta)], [D(\lambda), D(\beta)] \neq 0 \tag{A.3}$$

$$TrD(\lambda) = \pi\delta^{(2)}(\lambda) = \pi\delta(Re(\lambda))\delta(Im(\lambda)) \tag{A.4}$$

$$Tr[D(\lambda)D^{\dagger}(\beta)] = \pi\delta^{(2)}(\lambda-\beta) \tag{A.5}$$

$$D(\lambda)|\beta\rangle = |\lambda+\beta\rangle \exp[-\frac{1}{2}(\lambda\beta^{*}-\lambda^{*}\beta)] \tag{A.6}$$

$$\langle\alpha|D(\lambda)|\beta\rangle = \langle\alpha|\beta\rangle \exp[\lambda\alpha^{*}-\lambda^{*}\beta-1/2|\lambda|^{2}] \tag{A.7}$$

$$\langle n|D(\lambda)|\bar{n}\rangle = \sqrt{\frac{\bar{n}!}{n!}}\ \exp(-\lambda/2)\ \ \lambda^{n-\bar{n}}\ \ L_{\bar{n}}^{(n-\bar{n})}(|\lambda|^{2}) \qquad n \geq \bar{n} \tag{A.8}$$

$$\langle n|D(\lambda)|\bar{n}\rangle = \sqrt{\frac{n!}{\bar{n}!}}\ \exp(-\lambda/2)\ \ \lambda^{\bar{n}-n}\ \ L_{n}^{(\bar{n}-n)}(|\lambda|^{2}) \qquad \bar{n} \geq n \tag{A.9}$$

where $L_m^{(k)(x)}$ is is associated Laguerre polynomial.

$$L_m^{(k)}(x) = \sum_{n=0}^{m}(-1)^n\binom{m+k}{n+k}\frac{x^n}{n!}$$

A.3 Franck-Condon Factor for VSC and Bare Reactions

Franck-Condon factor for various combinations is given in Equation (2.8), here we will show the comparison of F-C for the VSC and bare case. As F-C for (0,1) is given as

$$F_{\chi,\bar{\chi}} = e^{(-S)}\ \ S_q, \qquad\qquad (\chi,\bar{\chi}) = (1_q,0),(0,1_q), \tag{A.10}$$

lets begin with VSC

$$F_{0,1_q} = e^{(-S)}\ \ S_q$$

$S = \sum_{q=1}^{N+1} Sq$ and $S_q = |\lambda_{Pq} - \lambda_{Rq}|^2$, where

$$\lambda_{Rq} = \lambda_R c_{qr}\omega_r/\omega_q$$

and

$$\lambda_{Pq} = \lambda_P c_{qr}\omega_r/\omega_q,$$

so we can write

$$|\lambda_{Pq} - \lambda_{Rq}|^2 = |\lambda_P \; c_{qr} \; \omega_r/\omega_q - \lambda_R c_{qr} \omega_r/\omega_q|^2 = |\lambda_P - \lambda_R|^2 \;\; |c_{qr}|^2 \;\; |\omega_r/\omega_q|^2$$

as $\omega_r \approx \omega_q$ so

$$|\lambda_{Pq} - \lambda_{Rq}|^2 = |\lambda_P - \lambda_R|^2 \;\; |c_{qr}|^2,$$

for any single mode q

$$F_{0,1_q} = \exp(S) \;\; |\lambda_P - \lambda_R|^2 \;\; |c_{qr}|^2. \tag{A.11}$$

In the case of bare i.e (0, 1r), $S_q \rightarrow S_r$ and $|c_{qr}|^2 \rightarrow |c_{1r}|^2$. Using these relation we can write

$$F_{0,1r} = \exp(S) \;\; |\lambda_P - \lambda_R|^2 \;\; |c_{1r}|^2,$$

as $|c_{1r}|^2 \approx 1$ so

$$F_{0,1r} \approx \exp(S) \;\; |\lambda_P - \lambda_R|^2. \tag{A.12}$$

Comparing Equation(A.11) and (A.12) we can write

$$F_{o,1q} \approx |c_{qr}|^2 \; F_{0,1r}$$

Appendix B

B.1 Numerical Simulation and Rate Calculations

Reaction rates are obtained by solving master equation numerically that aims to determine the population of reactants in for various time. The rate of change of population is given as $\frac{dP}{dt} = \mathcal{A}P$, where $\mathcal{A}$ is transition matrix and P is population vector. Population at ant time (t) is given as $P(t) = \exp(\mathcal{A}t)P(0)$. To determine the rate all of these parameters are converted into matrix form. We defined a matrix $B = M\mathcal{A}M^{-1}$, M being a diagonal matrix having diagonal elements $M_{(X,\chi),(X,\chi)} = f_{(X,\chi)}^{-1/2}$, where $f_{(X,\chi)} = \exp(-\beta E_{(X,\chi)})/\sum_{(X,\chi)} \exp(-\beta E_{(X,\chi)})$. After numerical diagonalization of B, at any time t population is given as

$$P(t) = M^{-1}\mathcal{Q}\exp(-Dt)\mathcal{Q}^T M P(0), \tag{B.1}$$

here eigenvectors of B are columns of matrix $\mathcal{Q}$ and eigenvalues are diagonal elements of diagonal matrix D. As we have assumed initial population is in reactant eigenstates so

$$P_{(R,\chi)}(0) = \frac{\exp(-\beta E_{(R,\chi)})}{\sum_\chi \exp(-\beta E_{R,\chi})} \tag{B.2}$$

$$P_{(P,\chi)}(0) = 0 \tag{B.3}$$

we than evaluate $P(t)$ at any time $t = J\Delta t$, keeping $\Delta t = 0.2ns$ and $J = 0, 1, ..., 100$. To obtained reaction rate we determined the reactant population

$$P_R = \sum_{\chi} P_{(R,\chi)},$$

and modeled it as

$$P_R = \exp(-\mathcal{Z}t)[]. \tag{B.4}$$

The fitting parameter $\mathcal{Z}$ is reaction rate.

Bibliography

[1] Kenji Hirai, James A Hutchison, and Hiroshi Uji-i. Recent progress in vibropolaritonic chemistry. *ChemPlusChem*, 2020.

[2] Thomas W Ebbesen. Hybrid light–matter states in a molecular and material science perspective. *Accounts of chemical research*, 2016.

[3] Raphael F Ribeiro, Luis A Martínez-Martínez, Matthew Du, Jorge Campos-Gonzalez-Angulo, and Joel Yuen-Zhou. Polariton chemistry: controlling molecular dynamics with optical cavities. *Chemical science*, 2018.

[4] VM Agranovich, Yu N Gartstein, and M Litinskaya. Hybrid resonant organic–inorganic nanostructures for optoelectronic applications. *Chemical reviews*, 2011.

[5] Manuel Hertzog, Mao Wang, Jürgen Mony, and Karl Börjesson. Strong light–matter interactions: a new direction within chemistry. *Chemical Society Reviews*, 2019.

[6] Bo Xiang and Wei Xiong. Molecular vibrational polariton: Its dynamics and potentials in novel chemistry and quantum technology. *The Journal of Chemical Physics*, 2021.

[7] Dominik Sidler, Michael Ruggenthaler, Christian Schäfer, Enrico Ronca, and Angel Rubio. A perspective on ab initio modeling of polaritonic chemistry: The role of non-equilibrium effects and quantum collectivity. *The Journal of Chemical Physics*, 2022.

[8] Anoop Thomas, Jino George, Atef Shalabney, Marian Dryzhakov, Sreejith J Varma, Joseph Moran, Thibault Chervy, Xiaolan Zhong, Eloïse Devaux, Cyriaque Genet, et al. Ground-state chemical reactivity under vibrational coupling to the vacuum electromagnetic field. *Angewandte Chemie*, 2016.

[9] Jyoti Lather, Pooja Bhatt, Anoop Thomas, Thomas W Ebbesen, and Jino George. Cavity catalysis by cooperative vibrational strong coupling of reactant and solvent molecules. *Angewandte Chemie*, 2019.

[10] Kenji Hirai, Rie Takeda, James A Hutchison, and Hiroshi Uji-i. Modulation of prins cyclization by vibrational strong coupling. *Angewandte Chemie*, 132(13):5370–5373, 2020.

[11] Hidefumi Hiura, Atef Shalabney, and Jino George. Vacuum-field catalysis: Accelerated reactions by vibrational ultra strong coupling. 2021.

[12] Jyoti Lather and Jino George. Improving enzyme catalytic efficiency by co-operative vibrational strong coupling of water. *The Journal of Physical Chemistry Letters*, 2020.

[13] Peter Hänggi, Peter Talkner, and Michal Borkovec. Reaction-rate theory: fifty years after kramers. *Reviews of modern physics*, 1990.

[14] Oksana Ostroverkhova. Organic optoelectronic materials: mechanisms and applications. *Chemical reviews*, 2016.

[15] Felipe Herrera and Jeffrey Owrutsky. Molecular polaritons for controlling chemistry with quantum optics. *The Journal of chemical physics*, 2020.

[16] Anoop Thomas, Lucas Lethuillier-Karl, Kalaivanan Nagarajan, Robrecht MA Vergauwe, Jino George, Thibault Chervy, Atef Shalabney, Eloïse Devaux, Cyriaque Genet, Joseph Moran, et al. Tilting a ground-state reactivity landscape by vibrational strong coupling. *Science*, 2019.

[17] Robrecht MA Vergauwe, Anoop Thomas, Kalaivanan Nagarajan, Atef Shalabney, Jino George, Thibault Chervy, Marcus Seidel, Eloïse Devaux, Vladimir Torbeev, and Thomas W Ebbesen. Modification of enzyme activity by vibrational strong coupling of water. *Angewandte Chemie International Edition*, 2019.

[18] Kenji Hirai, Hiroto Ishikawa, Thibault Chervy, James A Hutchison, and Hiroshi Uji-i. Selective crystallization via vibrational strong coupling. *Chemical science*, 2021.

[19] Javier Galego, Claudia Climent, Francisco J Garcia-Vidal, and Johannes Feist. Cavity casimir-polder forces and their effects in ground-state chemical reactivity. *Physical Review X*, 2019.

[20] Vladimir P Zhdanov. Vacuum field in a cavity, light-mediated vibrational coupling, and chemical reactivity. *Chemical Physics*, 535:110767, 2020.

[21] Xinyang Li, Arkajit Mandal, and Pengfei Huo. Cavity frequency-dependent theory for vibrational polariton chemistry. *Nature communications*, 2021.

[22] Tao E Li, Abraham Nitzan, and Joseph E Subotnik. On the origin of ground-state vacuum-field catalysis: Equilibrium consideration. *The Journal of chemical physics*, 2020.

[23] Eric W Fischer and Peter Saalfrank. Ground state properties and infrared spectra of anharmonic vibrational polaritons of small molecules in cavities. *The Journal of Chemical Physics*, 2021.

[24] Nguyen Thanh Phuc, Pham Quang Trung, and Akihito Ishizaki. Controlling the nonadiabatic electron-transfer reaction rate through molecular-vibration polaritons in the ultrastrong coupling regime. *Scientific reports*, 2020.

[25] Matthew Du, Jorge A Campos-Gonzalez-Angulo, and Joel Yuen-Zhou. Nonequilibrium effects of cavity leakage and vibrational dissipation

in thermally activated polariton chemistry. *The Journal of Chemical Physics*, 2021.

[26] Rudolph A Marcus. Chemical and electrochemical electron-transfer theory. *Annual review of physical chemistry*, 1964.

[27] Joshua Jortner. Temperature dependent activation energy for electron transfer between biological molecules. *The Journal of Chemical Physics*, 1976.

[28] Girish S Agarwal. *Quantum optics*. Cambridge University Press, 2012.

[29] Tomáš Neuman and Javier Aizpurua. Origin of the asymmetric light emission from molecular exciton–polaritons. *Optica*, 2018.

[30] Niclas S Mueller, Yu Okamura, Bruno GM Vieira, Sabrina Juergensen, Holger Lange, Eduardo B Barros, Florian Schulz, and Stephanie Reich. Deep strong light–matter coupling in plasmonic nanoparticle crystals. *Nature*, 2020.

[31] Marina Litinskaya, Peter Reineker, and Vladimir M Agranovich. Fast polariton relaxation in strongly coupled organic microcavities. *Journal of luminescence*, 2004.

[32] Matthew Pelton. Modified spontaneous emission in nanophotonic structures. *Nature Photonics*, 2015.

[33] Andrea B Grafton, Adam D Dunkelberger, Blake S Simpkins, Johan F Triana, Federico J Hernández, Felipe Herrera, and Jeffrey C Owrutsky. Excited-state vibration-polariton transitions and dynamics in nitroprusside. *Nature Communications*, 2021.

[34] Bo Xiang, Raphael F Ribeiro, Liying Chen, Jiaxi Wang, Matthew Du, Joel Yuen-Zhou, and Wei Xiong. State-selective polariton to dark state relaxation dynamics. *The Journal of Physical Chemistry A*, 2019.

[35] Chenru Duan, Qianlong Wang, Zhoufei Tang, and Jianlan Wu. The study of an extended hierarchy equation of motion in the spin-boson

model: The cutoff function of the sub-ohmic spectral density. *The Journal of Chemical Physics*, 2017.

[36] O Kühn and H Naundorf. Dissipative wave packet dynamics of the intramolecular hydrogen bond in o-phthalic acid monomethylester. *Physical Chemistry Chemical Physics*, 2003.